Published in Optics Letters 39, issue 1, 9-12, 2014
which should be used for any reference to this work

Ultrafast thin-disk laser with 80 μJ pulse energy and 242 W of average power

Clara J. Saraceno,[1,2,*] Florian Emaury,[1] Cinia Schriber,[1] Martin Hoffmann,[2] Matthias Golling,[1] Thomas Südmeyer,[2] and Ursula Keller[1]

[1]*Institute for Quantum Electronics, ETH Zurich, 8093 Zurich, Switzerland*

[2]*Laboratoire Temps-Fréquence, Université de Neuchâtel, 2000 Neuchâtel, Switzerland*

**Corresponding author: saraceno@phys.ethz.ch*

Received October 11, 2013; revised November 15, 2013; accepted November 15, 2013; posted November 15, 2013 (Doc. ID 199276); published December 16, 2013

We present a semiconductor saturable absorber mirror (SESAM) mode-locked thin-disk laser generating 80 μJ of pulse energy without additional amplification. This laser oscillator operates at a repetition rate of 3.03 MHz and delivers up to 242 W of average output power with a pulse duration of 1.07 ps, resulting in an output peak power of 66 MW. In order to minimize the parasitic nonlinearity of the air inside the laser cavity, the oscillator was operated in a vacuum environment. To start and stabilize soliton mode locking, we used an optimized high-damage threshold, low-loss SESAM. With this new milestone result, we have successfully scaled the pulse energy of ultrafast laser oscillators to a new performance regime and can predict that pulse energies of several hundreds of microjoules will become possible in the near future. Such lasers are interesting for both industrial and scientific applications, for example for precise micromachining and attosecond science.

OCIS codes: (140.3615) Lasers, ytterbium; (140.4050) Mode-locked lasers; (320.7090) Ultrafast lasers.

Ultrafast laser sources have advanced tremendously during the past two decades and have enabled important industrial and scientific breakthroughs [1]. There is a strong interest for a wide range of industrial and scientific applications to continue to push the performance of ultrafast sources toward higher average output powers at >100 kHz pulse repetition rates. Examples include laser precision micromachining and cutting [2,3], frequency metrology from the infrared to the extreme ultraviolet [4,5], and strong laser field physics in attosecond science [6,7].

Several laser technologies have, in the past years, successfully scaled the available average power of ultrafast systems. The most prominent examples are Innsolab amplifiers [8], chirped-pulse fiber amplifiers [9], and thin-disk laser (TDL) oscillators [10] and regenerative amplifiers [11]. Among these approaches, mode-locked TDLs can reach the targeted performance directly from a table-top oscillator without additional amplifiers. Since their first demonstration in the year 2000 [12], semiconductor saturable absorber mirror (SESAM)-mode-locked [13] TDLs [14] have set the frontiers in terms of average power and pulse energy available from ultrafast laser oscillators, reaching comparable levels to that of high repetition rate amplifier systems. In terms of average power, we have achieved up to 275 W from an Yb:YAG mode-locked oscillator, with 583-fs pulses at a repetition rate of 16.9 MHz, corresponding to 17 μJ of pulse energy [10]. This record-high average power was obtained by operating the oscillator in a vacuum environment, thus minimizing the parasitic nonlinearity of the atmosphere by several orders of magnitude. This was crucial to avoid an excessive nonlinear phase shift by self-phase modulation caused by the air inside the oscillator, which can destabilize mode-locked operation [15,16]. In terms of pulse energy, 41 μJ (Fig. 1, blue) have been previously demonstrated with a multipass Yb:YAG TDL. The parasitic nonlinearities were in this case reduced by using 11 double-passes through the Yb:YAG gain disk. This increased the overall gain per round trip, allowing to operate the oscillator at large output coupling rates and effectively reducing the intracavity peak power for a given output peak power. The average power obtained in this result was 145 W in 1.12-ps pulses [17].

Here, we present our latest milestone result (Fig. 1, red), where we successfully scaled the pulse energy of an Yb:YAG TDL to 80 μJ, which is the highest energy achieved directly from an ultrafast oscillator so far. Our laser operates at a repetition rate of 3.03 MHz and generates up to 242 W of average power. The pulses have a duration of 1.07 ps, resulting in an output peak power of 66 MW. The oscillator was operated in vacuum (≈1 mbar, limited by the vacuum pump) in order to reduce the nonlinear phase shift undergone by the pulses within one round trip in the laser oscillator, confirming the suitability of this approach [10] for pulse energy scaling of mode-locked oscillators.

The Yb:YAG thin disk (TRUMPF GmbH) had a thickness of <100 μm, a doping concentration of ≈10 at.%, was glued on a water-cooled diamond, and showed no significant thermal lensing throughout the pumping

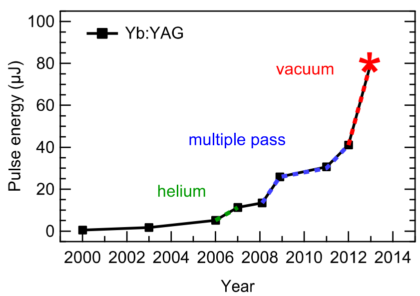

Fig. 1. Evolution of the maximum pulse energy available from mode-locked thin-disk oscillators since their first demonstration in the year 2000. The result presented in this Letter is highlighted with a red star symbol.

operation range of the laser (up to a pump power of 800 W). Without taking into account the extracted laser power, this corresponds to an intensity of ≈4.6 kW/cm^2. This enabled us to obtain robust fundamental mode operation throughout the entire pumping range, without the need to adapt any resonator length [18,19]. The pump spot on the disk had a diameter of 4.7 mm. The pump used was a commercially available fiber-coupled laser diode that can emit up to 1.2 kW of power at a wavelength of 940 nm. With 24 pump passes through the disk, we estimate a pump absorption of ≈90% at the inversion level used in this experiment.

The schematic layout of the oscillator can be seen in Fig. 2. Compared to our previous result [10], we increased the resonator length from 8.9 m (17 MHz) to ≈50 m (3 MHz) in order to achieve a higher pulse energy. A convenient way to increase the resonator length is to use of a Herriott-type multipass cavity (MPC) [20]. This type of MPC was already successfully implemented in mode-locked TDLs, and resulted in the first demonstration of an ultrafast oscillator with >10 μJ pulse energy in 2008 [21]. In these MPCs, the q-parameter of a Gaussian beam is kept unchanged, provided that the correct distance d between curved mirrors is chosen. Such an MPC can therefore be conveniently added to an existing laser cavity, without affecting mode sizes, thermal lens sensitivity, or operation in a given stability zone [22]. In our experiment, we chose an MPC based on a curved mirror with a radius of curvature of $R = 10$ m and eight passes on the curved surface. For more convenience and a smaller footprint, we folded the MPC with a flat mirror separated by a distance $d/2 = 1.45$ m to the curved mirror (Fig. 2, top). The addition of this MPC resulted in an extra cavity length of 23.4 m while keeping a reasonable footprint. In principle this footprint can be reduced further, for example by adding an extra folding flat mirror, or by implementing more advanced MPC arrangements.

In addition to adding this MPC, we geometrically increased the number of passes through the disk to two, further increasing our cavity length. The resulting increase in round trip gain allowed us to operate the oscillator efficiently at a higher degree of output coupling, while relaxing intracavity average power and intensities on critical components, such as the dispersive mirrors required for soliton mode locking. Such a multipass approach for reduction of the intracavity peak power was previously implemented and allowed to demonstrate a pulse energy >40 μJ [17]. However, in this previous result, the oscillator operated at atmospheric air pressure. Therefore, 11 gain double-passes on the disk were required to sufficiently reduce the intracavity peak power in order to avoid an excessive nonlinear phase shift of the pulses per round trip in the cavity. In contrast, we operate our oscillator in vacuum, thus reducing the nonlinearity of the ambient environment by several orders of magnitude. Therefore, we only use two double-passes on the gain disk, exclusively to limit intracavity average power and avoid thermal effects on critical intracavity components, in particular in the dispersive mirrors. Ongoing progress on the thermal management of these components will allow us to use even simpler oscillator geometries with one double-pass on the disk. For our experiment, we chose an output coupler of 25%. This value was chosen as a compromise between optical-to-optical efficiency and tolerable thermal effects on intracavity components.

The vacuum chamber was operated at 1 mbar of air pressure. The remaining air in the oscillator was the main contribution to the phase shift due to self-phase

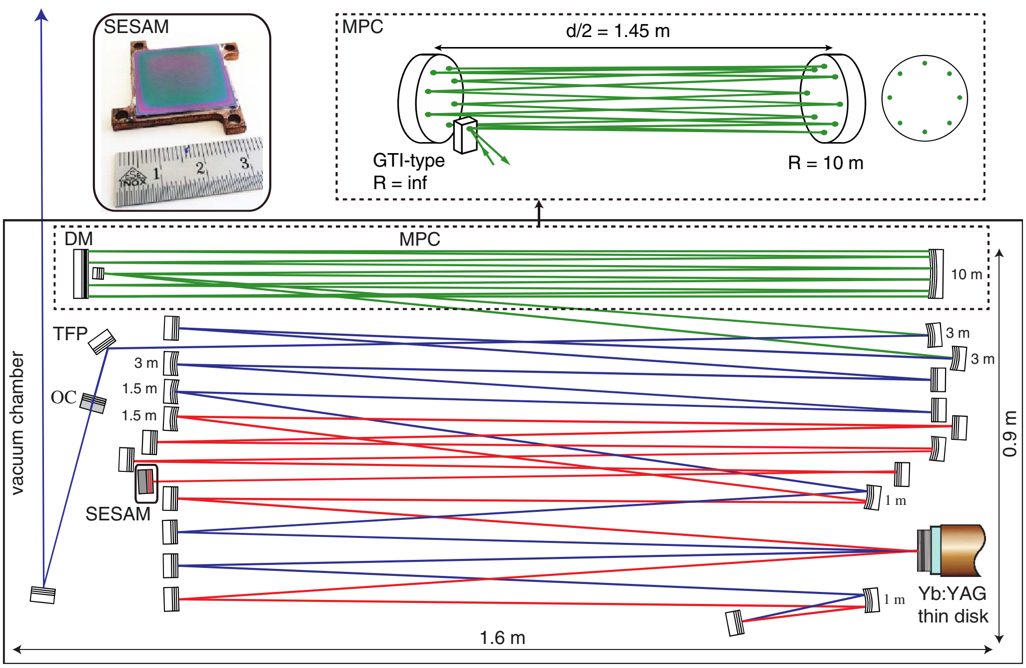

Fig. 2. Schematic of the 3.03 MHz mode-locked oscillator that delivers a pulse energy of 80 μJ. SESAM, semiconductor saturable absorber mirror; OC, output coupler; DM, dispersive mirror; TFP, thin-film polarizer; MPC, multipass cell; GTI, Gires–Tournois interferometer type dispersive mirror.

modulation of the pulses over one round trip in the laser cavity. For soliton mode locking [15,16] we introduced a total amount of dispersion per round trip of $\approx -28,000$ fs^2. This amount of negative dispersion was conveniently introduced by using a flat Gires–Tournois interferometer (GTI)-type dispersive mirror in the MPC (Fig. 2). For starting and stabilizing the soliton mode-locking mechanism, we used a SESAM especially designed for high damage threshold and high-power operation following our guidelines [23]. The spot radius on the SESAM in our laser cavity was ≈1 mm. Its design and growth temperature is the same as the one used in [10]. It consists of a 30-pair AlAs/GaAs distributed Bragg reflector, an antiresonant absorber section (three InGaAs quantum well absorbers grown at ≈300 °C), and a three-pair dielectric top-coating (SiO_2/Si_3N_4). As discussed in [23], this results in samples with low losses, a reflectivity rollover shifted to high fluences and high damage thresholds, all crucial aspects for average power and pulse energy scaling. We measured the nonlinear reflectivity and extracted the relevant parameters of this SESAM using a high-precision nonlinear reflectivity setup [24] seeded by an Yb:YAG TDL that delivers up to 2 µJ of pulse energy in 1-ps pulses at a repetition rate of 3.9 MHz. This allowed us to characterize our sample at parameters that are very close to the operation parameters of our TDL (pulse duration, repetition rate, and center wavelength). The measurement and corresponding least-squares fit >are presented in Fig. 3. The extracted parameters are a saturation fluence $F_{\text{sat}} = 120\ \mu\text{J/cm}^2$, a modulation depth $\Delta R = 1.1\%$, negligible nonsaturable losses $\Delta R_{\text{ns}} < 0.1\%$, and an induced absorption coefficient $F_2 \approx 7500\ \text{mJ/cm}^2$.

Mode-locked operation was obtained starting with 66 W of average output power (corresponding to a pulse energy of 22 µJ) and continued up to 242 W (corresponding to 80 µJ of pulse energy). As expected for soliton mode locking, the pulse duration decreased following a $1/E_p$ law from 2.80 to 1.07 ps (Fig. 4, left). At the maximum output power, the pump power was 790 W, resulting in an optical-to-optical efficiency ($P_{\text{out}}/P_{\text{pump}}$) of ≈30% (Fig. 4, right). At the maximum output power, the pulse energy reaches 80 µJ, a new breakthrough for ultrafast oscillators. At this maximum pulse energy the pulses have a full width half-maximum duration of 1.07 ps and a spectral width of 1.4 nm (Fig. 5, top), resulting in a peak power of 66 MW. The resulting time bandwidth product of 0.39 (an ideal transform-limited sech^2 pulse has 0.315)

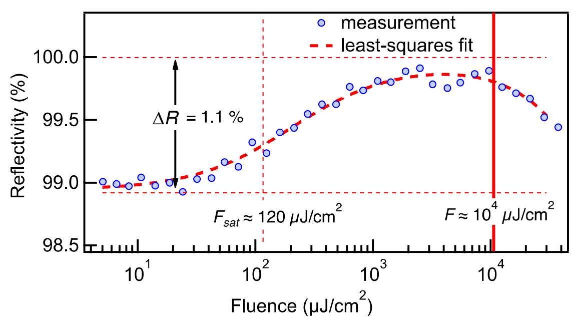

Fig. 3. Nonlinear reflectivity of the SESAM used for the high-energy TDL and corresponding least-squares fit. The operation fluence of this SESAM at the maximum output pulse energy of our high-energy TDL is marked in red.

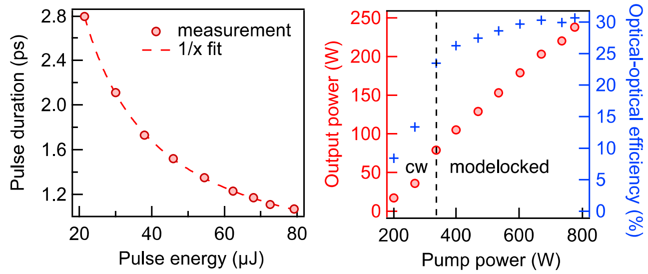

Fig. 4. Left: Duration of mode-locked pulses as a function of their output pulse energy. Right: Output power slope and optical-to-optical efficiency of the mode-locked oscillator.

indicates slightly chirped pulses, which was most likely induced by the strong saturation of the SESAM (≈90 times above the saturation fluence).

At the highest pulse energy, the radio-frequency spectrum of the pulses in a 16 MHz frequency span (Fig. 5, middle left) shows no parasitic side peaks, and no modulation of the harmonics of the fundamental repetition rate, confirming clean mode locking. A zoom around the main oscillation peak (Fig. 5, middle right), shows small relaxation oscillations with a suppression of ≈60 dB. However, the precise determination of the magnitude of these sidebands was limited in our experiment by the available resolution bandwidth of our radio-frequency spectrum analyzer (1 kHz). A full characterization of the noise properties of this oscillator is currently in progress, which will give us further insight on the influence of these relaxation oscillations and the noise of our oscillator. At the maximum output power, the beam was close to the diffraction limit with a measured $M^2 < 1.05$ (Fig. 5,

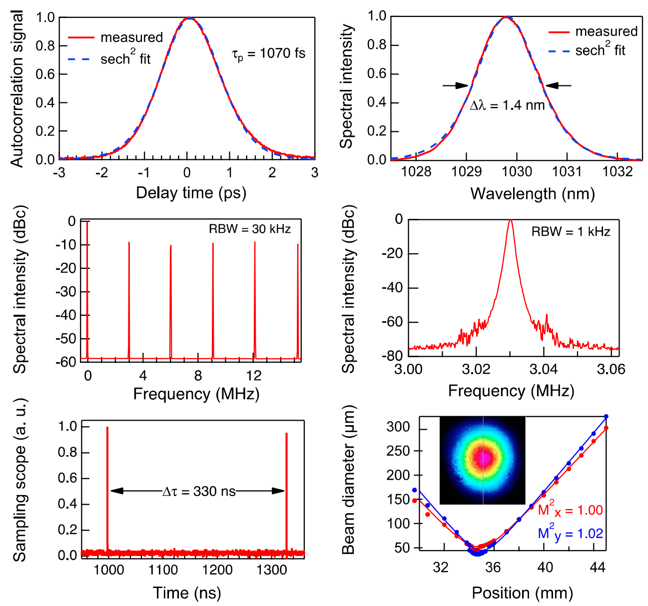

Fig. 5. Top: Autocorrelation (left) and optical spectrum (right) of the pulses and corresponding sech^2 fits. Middle: RF spectrum with a 16 MHz span and a RBW of 30 kHz (left) and with a 60 kHz span with a RBW of 1 kHz (right). Bottom: Sampling oscilloscope trace (left) and M^2 measurement performed using a commercially available scanning-slit automatized beam profiler and a focal length of $f = 100$ mm (right). All data was taken at the maximum pulse energy of 80 µJ.

bottom right). In addition, single-pulsed operation was confirmed with a sampling oscilloscope and a fast photodiode (45 GHz) (Fig. 5, bottom left) and by scanning the autocorrelator (scanning range 20 ps) in search for parasitic cross correlations with the main pulse. This additional check is important because oversaturated SESAMs tend to support multiple pulse operation that is difficult to see on an autocorrelator or optical spectrum analyzer alone [25]. A higher output power was prevented by the onset of mode-locking instabilities, which we believe originate in the strong saturation level of our SESAM. A lower degree of SESAM saturation with a larger spot size will allow us to reach higher average powers and higher pulse energies. In order to achieve this, we plan to use large SESAMs (>1 cm) with better flatness and heat removal in the future. Additional potential SESAM issues at such high intracavity peak and average power levels will be investigated in more details taking into account previous studies [23,26]. In addition, a lower degree of saturation should allow us to reach shorter pulses. We believe pulse durations in the 600 fs range should be feasible using Yb:YAG. Furthermore, even shorter pulses well below the sub-100-fs regime have recently been demonstrated in this laser geometry [27] using other novel broadband Yb-doped gain materials. This seems to indicate that extending this record high-energy performance to this pulse duration regime should be within reach, as the quality of these new gain materials progresses [28]. Furthermore, higher pulse energies can be reached by further extending the cavity length, for example with a different MPC design or by adding a second MPC in the resonator.

In summary, we presented a SESAM-mode-locked Yb:YAG TDL delivering pulses with 80 μJ pulse energy and an average power of 242 W. The pulses had a duration of 1.07 ps and the oscillator operated at a repetition rate of 3.03 MHz. To our knowledge, this represents the highest pulse energy ever obtained from a mode-locked laser oscillator to date. This result paves the way to ultrafast oscillators with hundreds of microjoules of pulse energy and hundreds of megawatts of peak power. In addition, pulse compression of this source will enable us to drive strong-field laser physics experiments at high-repetition rate directly from a table-top source.

This work was supported by the Swiss National Science Foundation (SNSF). Thomas Südmeyer acknowledges support from the ERC (Starting Grant 2011 #279545).

References

1. U. Keller, Appl. Phys. B **100**, 15 (2010).
2. L. Shah, M. E. Fermann, J. W. Dawson, and C. P. J. Barty, Opt. Express **14**, 12546 (2006).
3. A. Ancona, S. Doring, C. Jauregui, F. Roser, J. Limpert, S. Nolte, and A. Tunnermann, Opt. Lett. **34**, 3304 (2009).
4. A. Cingoz, D. C. Yost, T. K. Allison, A. Ruehl, M. E. Fermann, I. Hartl, and J. Ye, Nature **482**, 68 (2012).
5. I. Pupeza, S. Holzberger, T. Eidam, H. Carstens, D. Esser, J. Weitenberg, P. Russbueldt, J. Rauschenberger, J. Limpert, T. Udem, A. Tünnermann, T. W. Hansch, A. Apolonski, F. Krausz, and E. Fill, Nat. Photonics **7**, 608 (2013).
6. T. Südmeyer, S. V. Marchese, S. Hashimoto, C. R. E. Baer, G. Gingras, B. Witzel, and U. Keller, Nat. Photonics **2**, 599 (2008).
7. M. Krebs, S. Hädrich, S. Demmler, J. Rothhardt, A. Zair, L. Chipperfield, J. Limpert, and A. Tunnermann, Nat. Photonics **7**, 555 (2013).
8. P. Russbueldt, T. Mans, J. Weitenberg, H. D. Hoffmann, and R. Poprawe, Opt. Lett. **35**, 4169 (2010).
9. T. Eidam, S. Hanf, E. Seise, T. V. Andersen, T. Gabler, C. Wirth, T. Schreiber, J. Limpert, and A. Tünnermann, Opt. Lett. **35**, 94 (2010).
10. C. J. Saraceno, F. Emaury, O. H. Heckl, C. R. E. Baer, M. Hoffmann, C. Schriber, M. Golling, T. Südmeyer, and U. Keller, Opt. Express **20**, 23535 (2012).
11. R. Fleischhaker, R. Gebs, A. Budnicki, M. Wolf, J. Kleinbauer, and D. Sutter, in *European Conference on Lasers and Electro-Optics*, Munich, Germany (2013).
12. J. Aus der Au, G. J. Spühler, T. Südmeyer, R. Paschotta, R. Hövel, M. Moser, S. Erhard, M. Karszewski, A. Giesen, and U. Keller, Opt. Lett. **25**, 859 (2000).
13. U. Keller, K. J. Weingarten, F. X. Kärtner, D. Kopf, B. Braun, I. D. Jung, R. Fluck, C. Hönninger, N. Matuschek, and J. Aus der Au, IEEE J. Sel. Top. Quantum Electron. **2**, 435 (1996).
14. A. Giesen, H. Hügel, A. Voss, K. Wittig, U. Brauch, and H. Opower, Appl. Phys. B **58**, 365 (1994).
15. F. X. Kärtner and U. Keller, Opt. Lett. **20**, 16 (1995).
16. R. Paschotta and U. Keller, Appl. Phys. B **73**, 653 (2001).
17. D. Bauer, I. Zawischa, D. H. Sutter, A. Killi, and T. Dekorsy, Opt. Express **20**, 9698 (2012).
18. C. R. E. Baer, C. Kränkel, C. J. Saraceno, O. H. Heckl, M. Golling, R. Peters, K. Petermann, T. Südmeyer, G. Huber, and U. Keller, Opt. Lett. **35**, 2302 (2010).
19. C. R. E. Baer, O. H. Heckl, C. J. Saraceno, C. Schriber, C. Kränkel, T. Südmeyer, and U. Keller, Opt. Express **20**, 7054 (2012).
20. D. Herriott, H. Kogelnik, and R. Kompfner, Appl. Opt. **3**, 523 (1964).
21. S. V. Marchese, C. R. E. Baer, A. G. Engqvist, S. Hashimoto, D. J. H. C. Maas, M. Golling, T. Südmeyer, and U. Keller, Opt. Express **16**, 6397 (2008).
22. V. Magni, J. Opt. Soc. Am. A **4**, 1962 (1987).
23. C. J. Saraceno, C. Schriber, M. Mangold, M. Hoffmann, O. H. Heckl, C. R. E. Baer, M. Golling, T. Südmeyer, and U. Keller, IEEE J. Sel. Top. Quantum Electron. **18**, 29 (2012).
24. D. J. H. C. Maas, B. Rudin, A.-R. Bellancourt, D. Iwaniuk, S. V. Marchese, T. Südmeyer, and U. Keller, Opt. Express **16**, 7571 (2008).
25. C. J. Saraceno, F. Emaury, C. Schriber, O. H. Heckl, C. R. E. Baer, M. Hoffmann, K. Beil, C. Kränkel, M. Golling, T. Südmeyer, and U. Keller, Appl. Sci. **3**, 355 (2013).
26. J. Aus der Au, D. Kopf, F. Morier-Genoud, M. Moser, and U. Keller, Opt. Lett. **22**, 307 (1997).
27. A. Diebold, F. Emaury, C. Schriber, M. Golling, C. J. Saraceno, T. Südmeyer, and U. Keller, Opt. Lett. **38**, 3842 (2013).
28. T. Südmeyer, C. Kränkel, C. R. E. Baer, O. H. Heckl, C. J. Saraceno, M. Golling, R. Peters, K. Petermann, G. Huber, and U. Keller, Appl. Phys. B **97**, 281 (2009).